Neurobiology of Aging 81 (2019) 47–57

Contents lists available at ScienceDirect

Neurobiology of Aging

journal homepage: www.elsevier.com/locate/neuaging

Mice heterozygous for the *Cdh23/Ahl1* mutation show age-related deficits in auditory temporal processing

Alice L. Burghard, Nazli P. Morel, Douglas L. Oliver*

Department of Neuroscience, University of Connecticut School of Medicine, Farmington, CT, USA

ARTICLE INFO

Article history:
Received 18 October 2018
Received in revised form 15 January 2019
Accepted 3 February 2019
Available online 30 May 2019

Keywords:
Hearing loss
Cadherin 23
Amplitude modulation following response
Aging
Hearing test
Temporal precision

ABSTRACT

A mutation in the *Cdh23* gene is implicated in both syndromic and nonsyndromic hearing loss in humans and age-related hearing loss in C57BL/6 mice. It is generally assumed that human patients (as well as mouse models) only have a hearing loss phenotype if the mutation is homozygous. However, a major complaint for patients with a hearing disability is a reduced speech intelligibility that may be related to temporal processing deficits rather than just elevated thresholds. In this study, we used the amplitude modulation following response (AMFR) to test whether mice heterozygous for $Cdh23^{735A>G}$ have an auditory phenotype that includes temporal processing deficits. The hearing of mice heterozygous for the $Cdh23^{735A>G}$ mutation was compared with age-matched mice homozygous for either the mutation or the wild type in 3 cohorts of mice of both sexes at 2-3, 6, and 12 months of age. The AMFR technique was used to generate objective hearing thresholds for all mice across their range of hearing and to test their temporal processing. We found a genotype-dependent hearing loss in mice homozygous for the mutation starting at 5–11 weeks of age, an age when mice on the C57BL/6 background are often presumed to have normal hearing. The heterozygous animals retained normal hearing thresholds up to one year of age. Nevertheless, the heterozygous animals showed a decline in temporal processing abilities at one year of age that was independent of their hearing thresholds. These results suggest that mice heterozygous for the *Cdh23* mutation do not have truly normal hearing.

1. Introduction

Age-related hearing loss can be devastating for affected individuals and their environment. It can lead to social withdrawal and depression (Rutherford et al., 2018). The prevalence of hearing loss increases with age. One gene that has been found to be involved in syndromic (Usher syndrome type 1D) and nonsyndromic hearing loss (DFNB 12) as well as age-related hearing loss is *Cadherin 23/Otocadherin* (*Cdh23*) (Bork et al., 2001; Kim et al., 2016). It codes for Cadherin 23, a glycoprotein necessary for both development and maintenance of the hair bundle and tip links of the hair cells and is therefore essential for mechanotransduction (Müller, 2008). A point mutation, *Ahl1* ($Cdh23^{735A>G}$), has been identified to cause age-related hearing loss in several inbred mouse strains, including C57BL/6 (Johnson et al., 1997; Noben-Trauth et al., 2003). Mice homozygous for this mutation show a progressive high-frequency hearing loss starting at about 3 months of age that eventually results in severe hearing loss at one year of age (Bowl and Dawson, 2015). Similar to the heterozygous carriers of the human mutations of *Cdh23*, mice heterozygous for this mutation are considered to be unaffected (Bork et al., 2001; Noben-Trauth et al., 2003), but this assumption may be false.

A common complaint of patients with age-related hearing loss is reduced speech intelligibility, especially in noisy environments. This phenomenon cannot be sufficiently explained by elevated hearing thresholds, but it may be related to a decline in the temporal processing abilities in those patients (Babkoff and Fostick, 2017; Fitzgibbons and Gordon-Salant, 1996; Robert Frisina and Frisina, 1997). Behavioral tests, such as the gap detection test, are usually used to assess temporal processing performance in humans (Gordon-Salant and Fitzgibbons, 1993). Unfortunately, they are very time consuming and therefore not performed during standard hearing tests. It is possible that animals heterozygous for *Ahl1* also may have auditory deficits that cannot be found using standard hearing tests (e.g., hearing thresholds). The standard electrophysiological test to assess auditory function in both humans and animals is the auditory brainstem response (ABR) measurement. Although this is a very well-established method, it has one big disadvantage: the threshold is determined by the subjective

* Corresponding author at: Department of Neuroscience, University of Connecticut School of Medicine, UConn Health, 263 Farmington Ave, Farmington, CT 06030-3401, USA. Tel.: +1 860-679-2241; fax: +1 860-679-8766.
E-mail address: doliver@uchc.edu (D.L. Oliver).

0197-4580/$ – see front matter © 2019 Elsevier Inc. All rights reserved.
https://doi.org/10.1016/j.neurobiolaging.2019.02.029

identification of the response (François et al., 2016). So, a more objective method is necessary, one that can test threshold and temporal processing.

The amplitude modulation following response (AMFR) allows for both objective measurement of hearing thresholds and assessment of temporal processing abilities. AMFR, also known as the envelope following response, was first suggested as a test for frequency-specific hearing thresholds by Kuwada et al. (1986) and can also be used to test for temporal processing abilities. Purcell et al. (2004) reported that envelope following responses predict gap detection performance in humans. Consequently, the AMFR may provide a good way to assess changes in temporal processing with age.

Here, we used AMFR to test mice heterozygous for the *Ahl1* mutation for their hearing performance including temporal processing at different ages. Their results were compared with mice carrying 2 alleles of the mutation or the wild type. For this purpose, we tested transgenic mice on a C57BL/6 background expressing channelrhodopsin that had not been previously genotyped for this mutation. We also tested a second C57BL/6 background strain created to remove the *Ahl1* mutation and replace it with the wild-type gene. Hearing thresholds of that strain were previously evaluated and showed a rescue of low hearing thresholds up to 18 months of age (Johnson et al., 1997). In addition, CBA/J mice were used for comparisons at one year of age as they are reported to retain low hearing thresholds up to an old age. Our results show that the hearing thresholds of the heterozygous mice at one year of age were comparable to those of younger ages and mice homozygous for the wild-type genotype ($Cdh23^{735G}$). Despite this, the heterozygous mice at one year of age had temporal processing deficits.

2. Materials and methods

2.1. Animal model

All experiments were performed in accordance with the institutional guidelines and the NIH Guide for the Care and Use of Laboratory Animals and were approved by the Animal Care and Use Committee at the University of Connecticut Health Center. Animals of either sex were used. They were housed and bred in the local animal facility and every care was taken to reduce the number of animals and to refine the protocol to reduce any suffering.

Three different mouse strains were used. Breeding pairs were purchased from Jackson Laboratory (Bar Harbor, ME, USA). Previous experiments used a mouse with a C57BL6 background to identify GABAergic neurons optogenetically where channelrhodopsin was expressed under the VGAT promoter (B6.Cg-Tg [Slc32a1-COP4*H134R/EYFP] 8Gfng/J; Jackson Stock #14548) (Ono et al., 2017) (Abbreviated here as VGAT.) Because mice with the C57BL6 background are known to have the mutation for age-related hearing loss (*Ahl1*), we bred these mice with B6.CAST-Cdh23Ahl+/Kjn (Stock #002756) mice (B6.CAST), as they are reported to not have an age-related hearing loss. The result of this breeding created a hybrid of both strains (VGAT × B6.CAST). Additional CBA/J mice were purchased from Jackson Laboratory (Stock #000656) and were used as a control group for the one-year-old cohort after acclimating to the facility. Each tested animal was either ear punched or tail snipped to obtain a DNA sample.

2.2. Group design

This cross-sectional study included mice of both sexes. B6.CAST and VGAT × B6.CAST mice with different genotypes (A/A, A/G, G/G) for the *Ahl1* point mutation ($Cdh23^{735A>G}$) were compared at different ages (5–11 weeks, 24–29 weeks, and 45–52 weeks). In the 1-year-old group, CBA/J mice were added as an additional aged-matched control group. In the youngest group tested, only the A/A and A/G genotypes were found in the experimental animals. The genotyping results were obtained routinely after the auditory phenotype had been assessed. The experimenter was therefore only aware of the age of the tested mouse and blinded to the genotype. The distribution of genotypes for each strain is given in Table 1.

2.3. Anesthesia and surgical procedures

All recordings were performed on anesthetized mice (90 mg/kg ketamine, 9 mg/kg xylazine, and 2.7 mg/kg acepromazine, i.m. or i.p.) located in a sound attenuated chamber (IAC, Bronx, NY, USA). If needed, supplemental doses of ½ of the initial dose were administered (i.m. or i.p.). The animals were placed on a heating pad coupled to a rectal thermometer and kept at 36 °C–38 °C (FHC, Bowdoin, ME, USA). Oxygen was provided via a nose cone at a flow rate of 0.5 L/min. To avoid dry corneas, artificial tear salve was applied to the eyes. Approximately every 30 minutes, the animal received warm saline (0.3 mL, s.c.). The anesthesia level was checked via the toe pinch reflex (~every 30 minutes) and through a continuous measurement of heart rate and O_2 saturation levels via a pulse oximeter (MouseOx, Starr Life Science Corp, PA, USA). Before the surgery, 0.03 mL lidocaine hydrochloride (1%, s.c.) was injected at the site of incision dorsal to the midbrain. A craniotomy was performed to place a recording electrode directly over the inferior colliculus (IC). After a midline incision of the skin, the skull was exposed and a small indentation was made with an electrical drill about 0.5–1 mm caudal to lambda on the right side. To avoid damage to the underlying brain tissue, the final step of the craniotomy was done with a manual drill bit matched to the stainless steel screw (#0–80) that was placed into the craniotomy.

2.4. Electrophysiological recordings

The screw placed above the right IC served as the vertex recording electrode for ABRs and AMFRs. The reference and ground electrodes were needle electrodes placed retroauricularly on the contralateral and ipsilateral sides, respectively. A speaker (Revelator R2904/7000-05 Tweeter, ScanSpeak, Denmark) was placed 9 cm above the animal's head. The sound system was calibrated from 122–46,387 Hz by using a 1/4″ microphone (Type 4135, Brüel & Kjaer, Naerum, Denmark) placed also at a distance of 9 cm. An RZ6 auditory processor (TDT, Tucker Davis Technology, Alachua, USA) was used for the generation of the acoustic stimuli, and a TDT RA4PA medusa preamp with TDT RA4LI low impedance headstage provided the input to the RZ6 for the signal acquisition. For the click-evoked ABR recording, 512 0.2 ms clicks with alternating polarity were delivered at a presentation rate of 21 Hz at 0–85 dB sound pressure level (SPL) in 5 dB steps using TDT BioSig software. The signal was bandpass filtered (300–3000 Hz), and the click threshold was determined to be the midpoint between the first stimulus intensity with a detectable ABR waveform and the last stimulus intensity without a detectable ABR waveform. For offline analysis, the recorded signal

Table 1
Genotype distribution according to background strain

Genotype	A/A	A/G	G/G	Total
Strain				
B6.CAST	3	13	5	21
VGAT × B6.CAST	15	6	0	21
CBA/CaJ	0	0	6	6
Total	18	19	11	48

This table shows that most of the B6.CAST mice had an A/G genotype, whereas the VGAT × B6.CAST mice had predominately an A/A genotype. All CBA/J mice had a G/G genotype.

was filtered (500–3000 Hz) and the individual peaks were determined at all suprathreshold stimulus intensities by an experienced observer. Unclear responses were resolved by consensus with a second experienced observer. AMFR recordings were used to obtain objective frequency-specific thresholds and to evaluate the temporal processing abilities of the mice. We used a custom software written in MATLAB and TDT RPvdsEX (Gongqiang Yu, UConn Health) based on the methods developed by Kuwada et al. (1986). The acoustic stimuli were generated digitally and delivered with a sample rate of 97.7 kHz. For the recording of the evoked potentials, the signals were sampled at a rate of 9.7 kHz.

To establish the audiogram, a narrowband noise carrier (0.3 octave bandwidth) was centered at 2–40 kHz and modulated by a 42.9 Hz sine wave, raised to exponent 8 (see Equation 1), where m is the modulation depth, n is the exponent (the power of the raised sine-wave dc-shift), and fm is the modulator's frequency. We chose a modulation frequency (MF) of 42.9 Hz as this frequency was a good compromise of speed and auditory structures involved in generating the signal. Higher modulation frequencies would have sped up the process, but it would limit the number of auditory structures that were able to follow the modulation. The AMFR to an MF of 42.9 Hz includes generators from the cochlea up the midbrain (Kuwada et al., 2002).

$$\mathrm{MT(t)} = 2^{*}\mathrm{m}^{*}(((1+\sin(2^{*}\pi^{*}\mathrm{fm}^{*}\mathrm{t}))/2)\text{^}\mathrm{n} - 0.5) + 1; \quad (1)$$

During the recording, the coherence (COH) between the recorded signal at the MF and the MF of the stimulus was calculated online using the "mscohere" function in MATLAB. The COH strength was determined using Equation 2 where COH is the magnitude squared COH value of the bin containing the MF, and N_{noise} and SD_{noise} correspond to the mean and standard deviation, respectively, of the noise floor (bins 5–10 to the right side of the MF).

$$\mathrm{CS} = (\mathrm{COH} - \mathrm{N_{noise}})/\mathrm{SD_{noise}}; \quad (2)$$

If the COH value was above 0.25 and the COH strength exceeded 3, or if COH was >0.50 for 5 consecutive blocks (1 block = 8 epochs, 1 epoch = 10 cycles or min 250 ms), it was considered to be a positive response to the stimulus. At least 5 sequential positive responses were required to "pass" at that SPL level. In that case, the intensity level was decreased by 5 dB SPL and the process was repeated until a response could no longer be obtained at that intensity level. The AMFR was considered to be absent ("fail") if 5 sequential positive responses were not obtained after the presentation of 350 epochs. Depending on the thresholds obtained with the click ABR measurements and the carrier frequency to be tested, we usually started our recordings at 60–90 dB SPL and then decreased the stimulus intensity by 5 dB steps. The AMFR threshold was considered to be the midpoint between the lowest stimulus intensity with a response and the highest stimulus intensity without a response.

To assess the temporal processing abilities, the carrier frequency with the lowest threshold was presented at 30 dB above threshold with varying modulation frequencies (17–544 Hz, 0.3 octave steps and randomized order). During the offline analysis, the accumulated signal (length of one block) was segmented into the length of an epoch. These epochs were then averaged together and further filtered (1 octave bandwidth at MF). From this, peak synchrony (PS) and amplitude were extracted. To extract PS, the averaged epochs of the stimulus and the recorded signal were both aligned and segmented into cycles, followed by a comparison of the stimulus and the recorded signal for each cycle (using Equation 3) where N is the total number of cycles of the stimulus, θi is phase (in radian) between the peak of the evoked potentials to the peak of the stimulus at ith cycle.

$$\mathrm{PS} = \mathrm{sqrt}\Big(\sum((\cos(\theta\mathrm{i}))\text{^}2\Big) + \sum((\sin(\theta\mathrm{i}))\text{^}2))/\mathrm{N}; \quad (3)$$

To extract the amplitude of the response, the cycles of the recorded signal were all averaged, and the maximum and minimum were determined to calculate the amplitude.

2.5. Software and code accessibility

The code for recording the AMFR was written in MATLAB and TDT RPvdsEX and requires the TDT hardware cited previously. The analysis code for the AMFR was written in MATLAB. Both programs are available on request.

2.6. DNA isolation

Genomic DNA was extracted by one of 2 methods. In the first, the tissue sample was incubated (ear punch or tail snip) with 100 μL 50 mM NaOH at ~95 °C for 15 minutes and then spun at 13,000 rpm at 4 °C for 5 minutes. This reaction was stopped with 10 μL of 1 M Tris-HCl (pH 8) followed by another spin. Alternatively, the DNA was extracted from the tissue sample using 100 μL lysis buffer (12.5 μL 10N NaOH, 2.0 μL 0.5 M EDTA, and 5 mL H2O) at ~97 °C for 30 minutes, vortexing the tube every 5 minutes. This reaction was stopped with 100 μL neutralization buffer (500 μL 0.5 M Tris HCl, pH 6.8, and 9.5 mL H2O) and followed by a 10 minutes spin at room temperature. The DNA thus extracted was further diluted 1:1 in water. All DNA samples were stored at −20 °C.

2.7. PCR and sequencing

For the PCR reaction, we used the GoTaq Flexi DNA polymerase kit (Promega, USA). We added 0.6 μL DNA to 19 μL reaction mix, which included 0.2 μL of each primer at a concentration of 20 μM. The following primer sequences were used: GTCTCCCAAGGATCAAGACAAG (forward) and CCACTGCTCTAAGGGAATCAAA (reverse). The final PCR product was purified using a column purification kit (GeneJET PCR Purification kit, Thermo Scientific, USA) and sequenced using Sanger sequencing (Genewiz LLC, South Plainfield, NJ, USA) and the forward primer.

2.8. Statistics

All statistical analyses, except the post hoc power analysis, were performed using Origin (OriginLab Corporation, Northampton, MA, USA). The power analysis was performed using G*Power 3.1 (Heinrich-Heine University, Düsseldorf, Germany). For the audiograms, a one-way analysis of variance (ANOVA) was performed at each individual frequency (and the click threshold). For the temporal processing analysis, a 2-way ANOVA using the factors MF and genotype was performed for each age. The amplitude growth functions for the one-year-old cohort were also analyzed using a 2-way ANOVA with genotype and intensity level as the 2 factors. Post hoc mean comparisons were done using the Scheffe test. If not stated otherwise, all tests were performed on mice with a C57BL/6 background only and did not include CBA/J mice.

All data not representing individual animals are plotted as mean ± SEM. Statistical results for the data shown can be found in the appendix. For statistical analysis of hearing performance, we compared mice of different genotypes within the C57BL/6 background if not stated otherwise.

3. Results

3.1. Genotyping

VGAT and B6.CAST mice were cross-bred to reduce the prevalence of the Ahl phenotype resulting from the *Cdh23* point mutation in chromosome 10 at position 753 in the genetically modified VGAT strain. All 3 genotypes (A/A, A/G, G/G) were found in mice of the B6.CAST strain. A representative example of all 3 genotypes in the sequencing results can be found in Fig.1. By chance, only A/G and A/A were found in mice tested at the youngest age. The offspring of the cross-breeding, the VGAT × B6.CAST mice, were predominately of the A/A genotype, but some mice were A/G. Every CBA/J mouse tested had the G/G genotype. An overview of the distribution of genotypes across strains is given in Table 1. In most cases, the acoustic recordings occurred before the tissue used for genotyping was obtained, so the investigators were blind to the genotype during the recording sessions.

The mice were separated into 3 cohorts depending on their age. The young group was 5–11 weeks old and consisted of 7 A/A and 6 A/G mice. The six-month-old group (24–29 weeks) consisted of 5 A/A, 8 A/G, and 2 G/G mice. The one-year old cohort (45–53 weeks) had 6 A/A, 4 A/G, and 3 G/G mice of a C57BL/6 background. In addition, 6 G/G mice with CBA/J background were tested at this age.

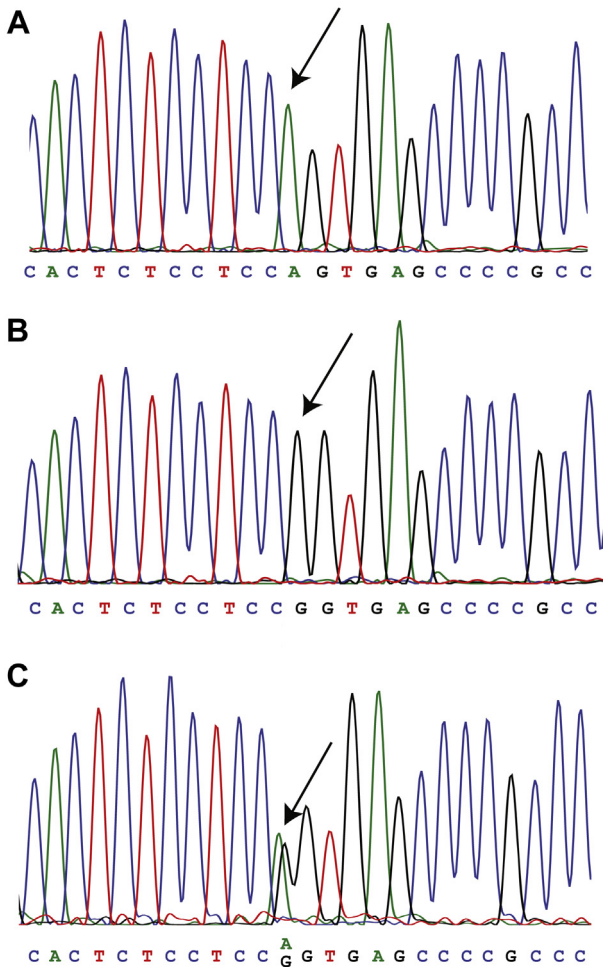

Fig. 1. Sequencing results of 3 representative animals with the arrows pointing at the point of interest. (A) The trace shows a clear peak for adenine (A), indicating that the animal is homozygous for the mutation. (B) This animal is homozygous for the wild-type gene as only a peak for guanine (G) can be seen. (C) The presence of a peak for both adenine and guanine classifies this animal as heterozygous.

3.2. Hearing thresholds

When we compared hearing thresholds, the *Cdh23* genotype was a better predictor of the audiogram than the strain. The hearing thresholds of B6.CAST and VGAT × B6.CAST at a young age (Fig. 2A and B) revealed lower thresholds for VGAT × B6.CAST mice at 16 kHz, but at other frequencies, there were no differences. There was no difference in click stimulus thresholds. Comparing the same animals grouped according to their genotype instead of strain (Fig. 2C and D) revealed no differences at 16 kHz, but a significantly higher threshold at 40 kHz for the A/A genotype. This grouping reveals a clear genotype-dependent high-frequency hearing loss, which is dissimilar to the strain-dependent results (please see Appendices Table A1 for statistical results). The observed strain differences at 16 kHz can be explained by the fact that the genotype distribution in the 2 groups varied (see Table 1). Although the click thresholds are nearly the same for both A/A and A/G mice in the young cohort, note that at 40 kHz, every single A/A mouse had a higher threshold than the A/G mice (Fig. 2C). Thus, the homozygous A/A genotype reveals a high-frequency difference even at 5–11 weeks when many investigators presume that mice on a C57Bl/6 background have normal hearing. For this reason, all further data are grouped according to genotype.

The genotype-dependent high-frequency hearing loss is even more pronounced in the comparison of 6-month-old mice. Although the click thresholds were similar, the A/A mice had significantly higher thresholds at 32 and 40 kHz compared with both A/G and G/G (Fig. 3A and B). High-frequency hearing in the A/G mice remains at the same levels as seen in the younger mice and is similar to the G/G mice (for statistical results, please see Appendices Tables A1-1 and A1-2).

In the one-year-old cohort, the A/A mice show clear hearing deficits across most of the audiogram and the click threshold (Fig. 3C and D). The heterozygous mice do not differ in their hearing phenotype from the G/G animals, both mice with B6.CAST and CBA/J background. There were significantly higher thresholds for A/A mice from 4–40 kHz. The click threshold only showed a significant threshold difference at this age with again the A/A mice having the highest thresholds. For exact statistical results, please see Appendices Table A1-1 (one-way ANOVA) and Table A1-2 (Scheffe test).

3.3. Temporal processing

We analyzed the temporal processing abilities of the mice using the AMFR data at the carrier frequency that corresponded to the most sensitive part of the audiogram for each individual mouse. The MF was varied from 17 to 544 Hz (3rd octave steps) at a stimulus intensity of 30 dB above threshold. For the oldest A/A mice, a 90 dB SPL sound intensity was used because the thresholds were too high to allow a 30 dB increase in several cases (30 dB above threshold: n = 2; 25 dB: n = 1; 20 dB: n = 1, 15 dB: n = 1, one mouse was excluded as 90 dB SPL did not elicit a strong enough response to all MF to pass criteria [threshold: 82.5 dB SPL]).

A clear influence of MF on peak amplitude is present for each age group and is depicted in Fig. 4. It can be clearly seen that as the MF increases, the amplitude of the AMFR decreases. A 2-way ANOVA confirmed a significant influence of MF at all ages (see Appendices Table A2-1; for post hoc analysis, see Table A2-2). This decrease in amplitude at higher modulation frequencies is an expected result because fewer neurons in the auditory system are able to follow the higher modulation frequencies. An influence of genotype on peak amplitude was not observed in any age group (CBA/J mice excluded), and there was no interaction between MF and genotype at any age (see Appendices Table A2-1).

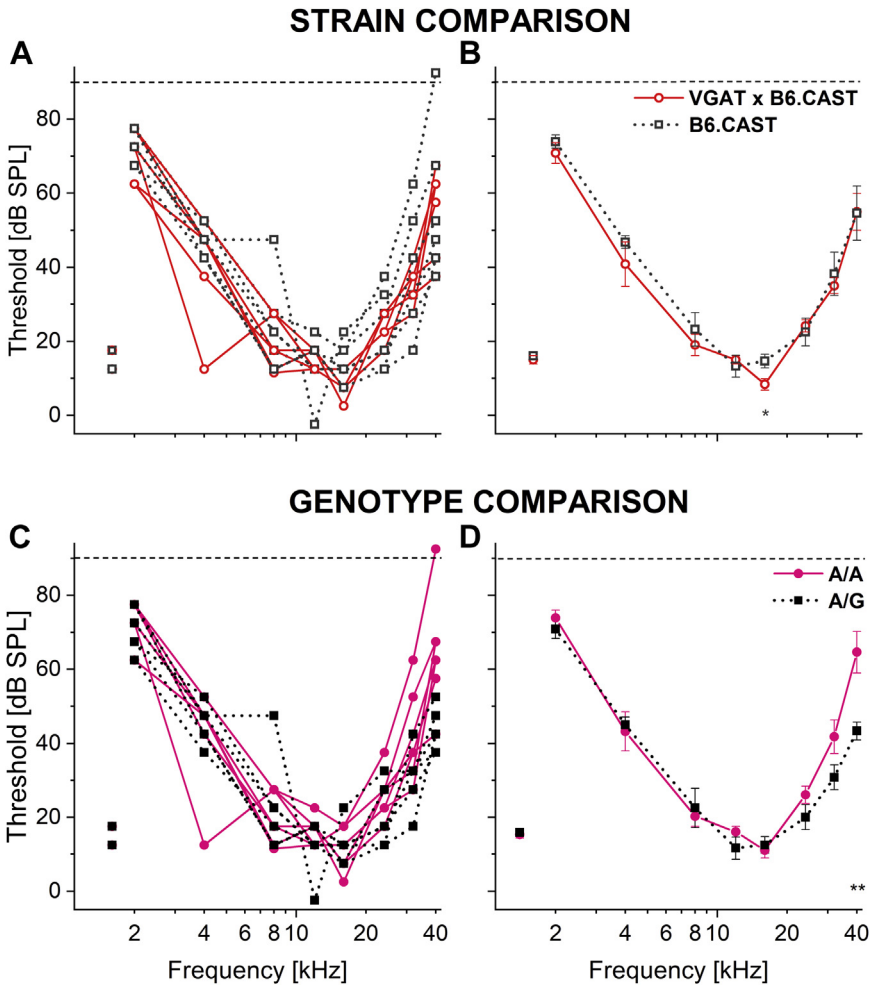

Fig. 2. Audiograms and click thresholds show a genotype-dependent phenotype at a young age. (A and B) Young animals sorted according to strain (VGAT × B6.CAST: n = 6, B6.CAST: n = 7). Red open circles represent VGAT × B6.CAST mice, dark gray open squares with dotted lines represent B6.CAST mice. (C and D) The same animals as in A + B are plotted according to genotype (A/A: n = 7 and A/G: n = 6). Magenta circles and solid lines indicate A/A mice, black squares and dotted lines indicate A/G mice. The left column shows individual animals; in the right column, the respective groups are plotted as mean ± SEM. The dashed line at 90 dB SPL indicates the maximum stimulus intensity used in this study. In cases in which no sound elicited a response, the threshold was assigned to be 92.5 dB SPL. *: $p < 0.05$, **: $p < 0.01$. For the statistical results, see Appendices Table A1-1.

The temporal precision of the AMFR was significantly influenced by both MF and genotype. The temporal precision of the AMFR was evaluated by measuring the PS of the repeated cycles of the response (Fig. 5). Similar to the results for peak amplitude, a significant influence of MF could be detected for all tested ages, but an interaction between genotype and MF was not detected at any age (for results of a 2-way ANOVA analysis, see Appendices: Table A3-1; for the post hoc analysis, see Table A3-2). Interestingly, the genotype was a major influence that was present for the 6-month-old and the 1-year-old cohorts (Fig. 5C–F). In the middle-aged cohort, the heterozygous animals show a slightly lower PS than the G/G mice (Fig. 5C and D). At one year of age, all 3 genotypes on a C57BL/6 background show a decrease in PS at higher modulation frequencies compared with CBA/J mice (Fig. 5E and F).

Besides the background strain difference, we also found a *Cdh23* genotype-dependent influence on PS (Appendices Tables A3-1 and A3-2). Remarkably, the cohort of one-year-old A/G mice with apparently "normal hearing" showed a clear deficit in temporal precision at high modulation frequencies compared to both other genotypes. This was surprising as their hearing thresholds are much better than for the age-matched A/A mice and did not differ from the G/G mice. This suggests that there are deficits in temporal processing abilities in the heterozygous mice despite their relatively normal audiograms. Altogether, this argues that the $Cdh23^{753A>G}$ mutation adds to another strain-dependent temporal processing difference in these mice. To establish that this effect is not due to the small sample size, we performed a post hoc power analysis and verified that the F-values indeed exceeded the critical F-value (1.29), resulting in a power of >0.99.

To remove the influence of threshold on testing the temporal processing abilities, we stimulated each mouse at the same sensation level, for example, 30 dB above threshold. Moreover, the hearing thresholds of the $Cdh23^{735A/G}$ mice were comparable both to younger genotype-matched mice and to the age-matched $Cdh23^{735G/G}$ mice, emphasizing that this temporal processing deficit is threshold independent. The fact that the C57BL/6 $Cdh23^{735A/A}$ mice did not show such severe temporal deficits might be due to the fact that in those mice, we were not able to always stimulate 30 dB above threshold.

3.4. Intensity coding

It was possible that this unexpected finding in temporal processing was accompanied by a difference in intensity coding. To

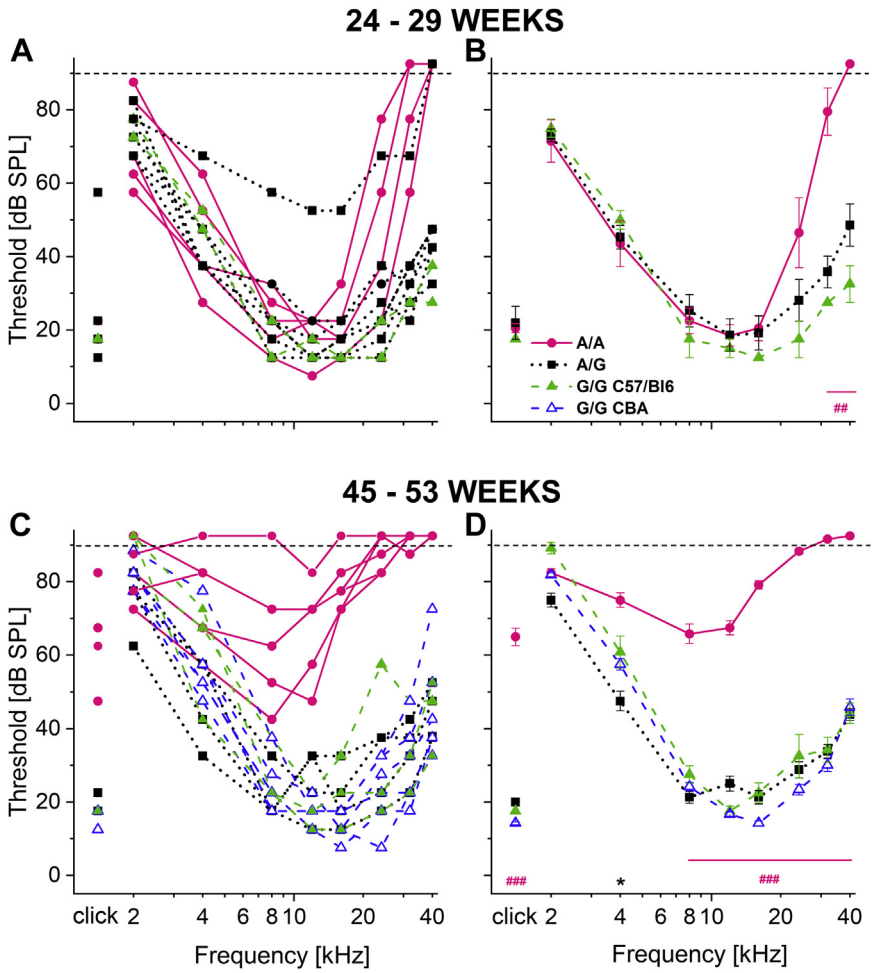

Fig. 3. Audiograms of the middle and older aged cohort reveal a clear genotype-dependent hearing loss. (A and B) The 6-month-old mice (A/A: n = 5, A/G: n = 9, and G/G: n = 2). (C and D) One-year-old cohort mice (A/A: n = 4, A/G: n = 4, and G/G: B6.CAST: n = 3, CBA/J: n = 6). The left column shows individual animals; in the right column, the respective groups are plotted as mean ± SEM. Maximum stimulus level 90 dB SPL. The blue open triangles represent the G/G mouse with CBA/J background; the other color codes, symbols, and significance values as in Fig. 2C–D. *: $p < 0.05$, #: statistical result between A/A and both A/G and G/G. ##: $p < 0.01$, ###: $p < 0.001$. For the statistical results, see Appendices Table A1-1 (1-way ANOVA) and Table A1-2 (Scheffe test).

investigate this, we analyzed the growth function of the AMFR peak amplitude relative to increasing sound intensity in mice at one year of age. Fig. 6A–C shows plots of the AMFR amplitude growth function at the same carrier frequency used for the temporal processing. It can be clearly seen that most of the A/A mice had a much higher hearing threshold than all other mice (Fig. 6A, D, G and J) and therefore a direct comparison of amplitude growth (slope) was easier if it was done if the amplitude growth was compared at dB above threshold (= sensation level) (Fig.6 middle and right column). This analysis, however, showed no difference between A/G and G/G mice. On the other hand, the slope of the A/A mice was steeper and reached higher amplitudes than both other genotypes, even at lower levels relative to threshold (Fig.6B and C). In the A/A group, the maximum response amplitude was reached already at 12.5 dB above threshold for one animal and at 27.5 dB above threshold for another animal (Fig. 6A). This shows that the very high hearing thresholds of the A/A mice can produce an AMFR amplitude that is as large or larger than of animals with lower thresholds but over a more limited range of intensities. This suggests a possible increase in central gain after hearing loss that could be related to hyperacusis, as Hickox and Liberman, 2014 have shown that central gain after noise exposure can lead to increased startle responses in mice.

To investigate if this difference in the amplitude growth function is uniformly present at different stations of the auditory brainstem, we analyzed the amplitude growth of peaks I, III, and V of the click-evoked ABR of animals at one year of age (Fig. 6D–L). The growth function for peak I, that represents cochlear activity (Fig. 6D–F), showed a significantly greater amplitude (growth) for aged CBA/J mice compared to all mice on a C57BL/6 background but no differences within the different C57BL/6 genotypes (see Appendices Tables A4-1, A4-2 and A4-3). The A/A mice did not differ in their peak I amplitude growth compared with the A/G or G/G (C57BL/6) mice (Appendices Table A4-1), although their thresholds did differ significantly (Figs. 3 and 6D). The growth curve for peak III, presumably from the superior olivary complex, showed a similar pattern as for peak I, although the difference between the CBA/J mice and the C57BL/6 mice was reduced but still significant (see Appendices Tables A4-1 and A4-3). Comparing the different genotypes of the C57BL/6 mice revealed no significant difference between the genotypes (see Appendices Tables A4-1, A4-2 and A4-3). At peak V, a signal presumed to come from the IC, a genotype-dependent phenotype is still present, but it changed (Fig. 6J–L). Here, the A/A mice had significantly larger amplitudes compared to the G/G mice of the C57BL/6 background but not compared to the CBA/J mice. The G/G mice of the 2 different background strains on the other hand did differ significantly in their amplitude growth function with the C57BL/6 mice, showing the shallower growth curve (see Appendices Tables A4-1, A4-2 and A4-3). These data

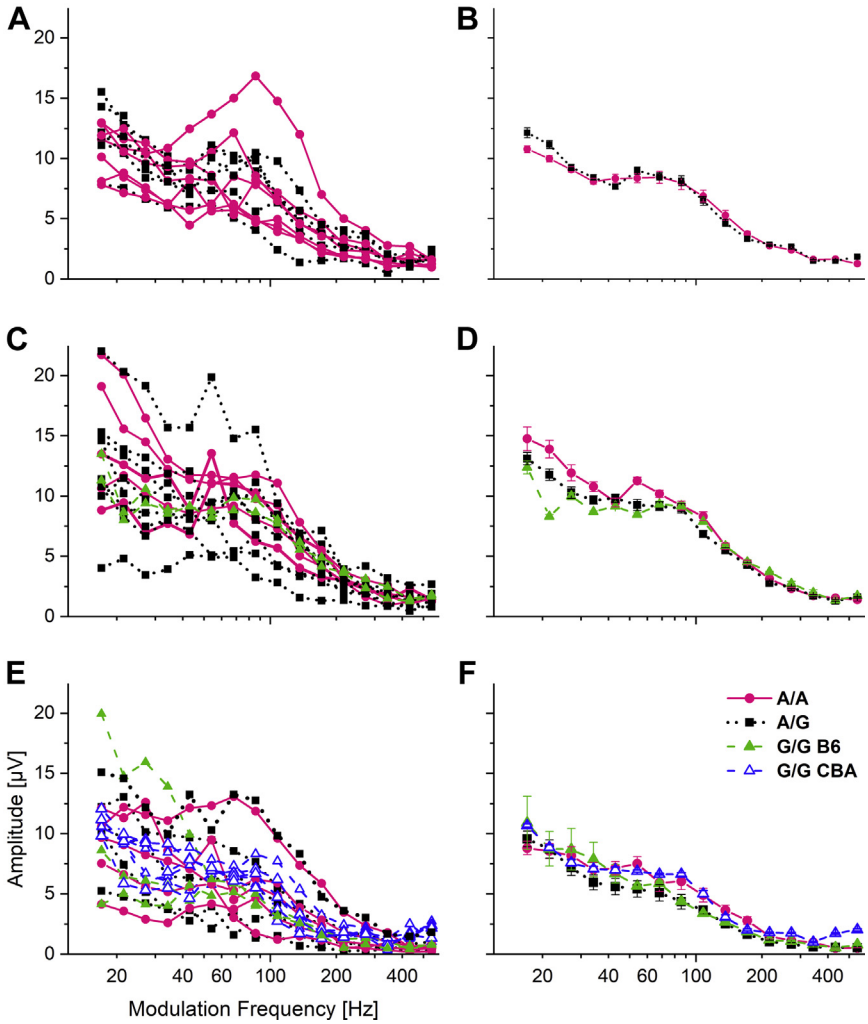

Fig. 4. Amplitude modulation following response (AMFR) peak amplitude for different modulation frequencies at 30 dB above threshold at most sensitive carrier frequency shows a decline at high modulation frequencies. A clear influence of modulation frequency is present for each age group. A genotype-dependent difference is present only for the oldest tested group. The left column shows individual animals; in the right column, the respective groups are plotted as mean ± SEM. (A and B) 5- to 11-week-old mice (A/A: n = 7 and A/G: n = 6); (C and D) 24- to 29-week-old mice (A/A: n = 5, A/G: n = 9, and G/G: n = 2); (E and F) 45- to 53-week-old mice (A/A: n = 5, A/G: n = 4, G/G: n = 3 [C57Bl/6] + 6 [CBA/J]). In this age group, A/A mice were stimulated at 90 dB SPL (<30 dB above threshold in 3 animals). Color codes and symbols as in Fig. 2C–D. For the statistical results, see Appendices Table A2-1 (2-way ANOVA) and Table A2-2 (Scheffe test for post hoc comparison of genotypes).

suggest that differences in intensity coding with aging are more related to the strain of the mouse than the *Cdh23*$^{753A>G}$ genotype.

4. Discussion

The present study shows that using AMFR measurements allowed us to detect a previously unknown temporal processing deficit in mice heterozygous for the *Ahl1* (*Cdh23*$^{735\ A>G}$) mutation. This deficit was independent of hearing thresholds.

4.1. Sensitivity and objectivity of AMFR for threshold measurements

The AMFR technique has a greater sensitivity and objectivity than other methods to obtain audiograms. An AMFR signal obtained with a 42.9 Hz MF includes activity from the cochlea up to the IC, whereas the AMFR to lower modulation rates also contains signals from the thalamus and cortex (Kuwada et al., 2002). The tone pip-evoked ABR is a well-established procedure to obtain audiograms in a variety of species, but its analysis is subjective (François et al., 2016). This explains why hearing thresholds measured with the tone pip ABR often do not match those obtained with behavioral tests (Radziwon et al., 2009). The AMFR was suggested as a diagnostic test by Kuwada et al., 1986; it is often called the envelope following response and is commercially available in advanced test equipment for clinical audiology. Several studies have shown that the AMFR method yields thresholds similar to behavioral thresholds (Aoyagi et al., 1994; Griffiths and Chambers, 1991). Our custom software for the AMFR method has the advantage of being independent of the previous experience of the experimenter, and it is a truly objective test. Predetermined criteria were used to define a positive response in the EEG to the MF where the signal was significantly above the noise floor and had to be present 5 times without interruption.

The AMFR method may be especially useful in the assessment of temporal processing in relation to genetic abnormalities. Gap detection is the behavioral test usually performed to evaluate temporal processing abilities (Harris et al., 2010). Williamson et al., 2015 proposed to use gap-in-noise ABR measurements instead of behavioral experiments. Although this method also allows the detection of temporal processing deficits, it still has the disadvantage of all ABR recordings—the need to reliably identify the respective peaks. The AMFR on the other hand is faster than

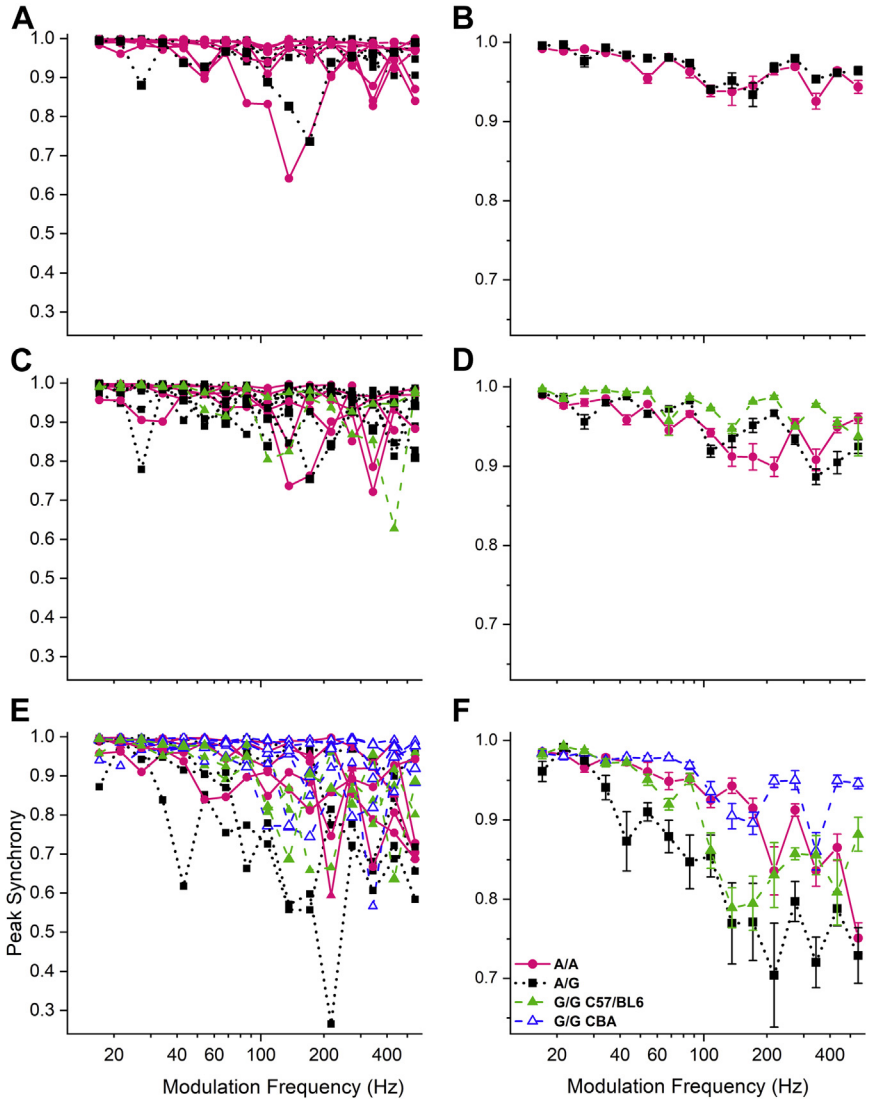

Fig. 5. Amplitude modulation following response (AMFR) peak synchrony as a measure for temporal precision reveals deficits in the one-year-old heterozygous animals. The peak synchrony is plotted as a function of modulation frequency in the 1-year-old cohort. A significant influence of genotype is seen. A strain difference between CBA/J and C57Bl/6 mice is also present for matched G/G *Cdh23* genotype. (A and B) 5- to 11-week-old mice (A/A: n = 7, A/G: n = 6); (C and D) 24- to 29-week-old mice (A/A: n = 5, A/G: n = 9, and G/G: n = 2); (E and F) 45- to 53-week-old mice (A/A: n = 5, A/G: n = 4, and G/G: n = 6 [CBA/J] + 3 [B6.CAST]). In this age group, A/A mice were stimulated at 90 dB SPL (<30 dB above threshold in 3 animals). Color codes and symbols as in Fig. 2C–D. For the statistical results, see Appendices Table A3-1 (2-way ANOVA) and Table A3-2 (Scheffe test for post-hoc comparison of genotypes).

behavioral testing and more objective than ABR peak analysis and can also predict the outcome of gap detection (Purcell et al., 2004). Thus, the AMFR is highly desirable as a fast clinical screening tool for temporal processing disorders.

4.2. Strain differences

Aging may further accentuate differences between strains of mice. At one year of age, the amplitude growth of ABR wave I in relation to sound intensity revealed differences between the mouse strains but not the *Cdh23*^{735} genotype (Fig. 6). The growth function for the *Cdh23*$^{735G/G}$ mice on the CBA background was steep, but flatter for all 3 *Cdh23*^{735} genotypes on the C57BL/6 background. Such difference in intensity coding at the level of the auditory nerve may be further evidence of additional loci in the C57BL/6 genome, influencing the hearing phenotype as already suggested (Johnson et al., 2017). A study by Frisina et al., 2007 reported a reduced activity of the medial olivocochlear efferent system in young adult C57 mice compared to age-matched CBA mice, indicating further strain differences in different parts of the auditory system besides the cochlea. The amplitude growth functions of the later ABR waves (click evoked) and the AMFR (42.9 Hz MF) were more similar between strains and suggests that this intensity coding deficit is, at least partially, compensated by central gain mechanisms. Such a phenomenon of central gain is also observed in other models of aging and models of cochlear synaptopathy (Chambers et al., 2016; Parthasarathy et al., 2019). Cochlear synaptopathy (e.g., the loss of the synapse between inner hair cell and auditory nerve fiber) is usually accompanied by a reduction in ABR peak I amplitude and an increase in the amplitude ratio of peaks V to I (Sergeyenko et al., 2013). After the loss of synaptic input, a degeneration of spiral ganglion cells (SGCs) is observed. However, the age of onset and extend of this SGC loss is different between C57BL/6 mice and CBA mice [~20% at 3 months of age for C57BL/6 (Hequembourg and Liberman, 2001) and <10% at ~3 months of age in CBA/CaJ mice (Sergeyenko et al., 2013)]. It is therefore possible that the observed

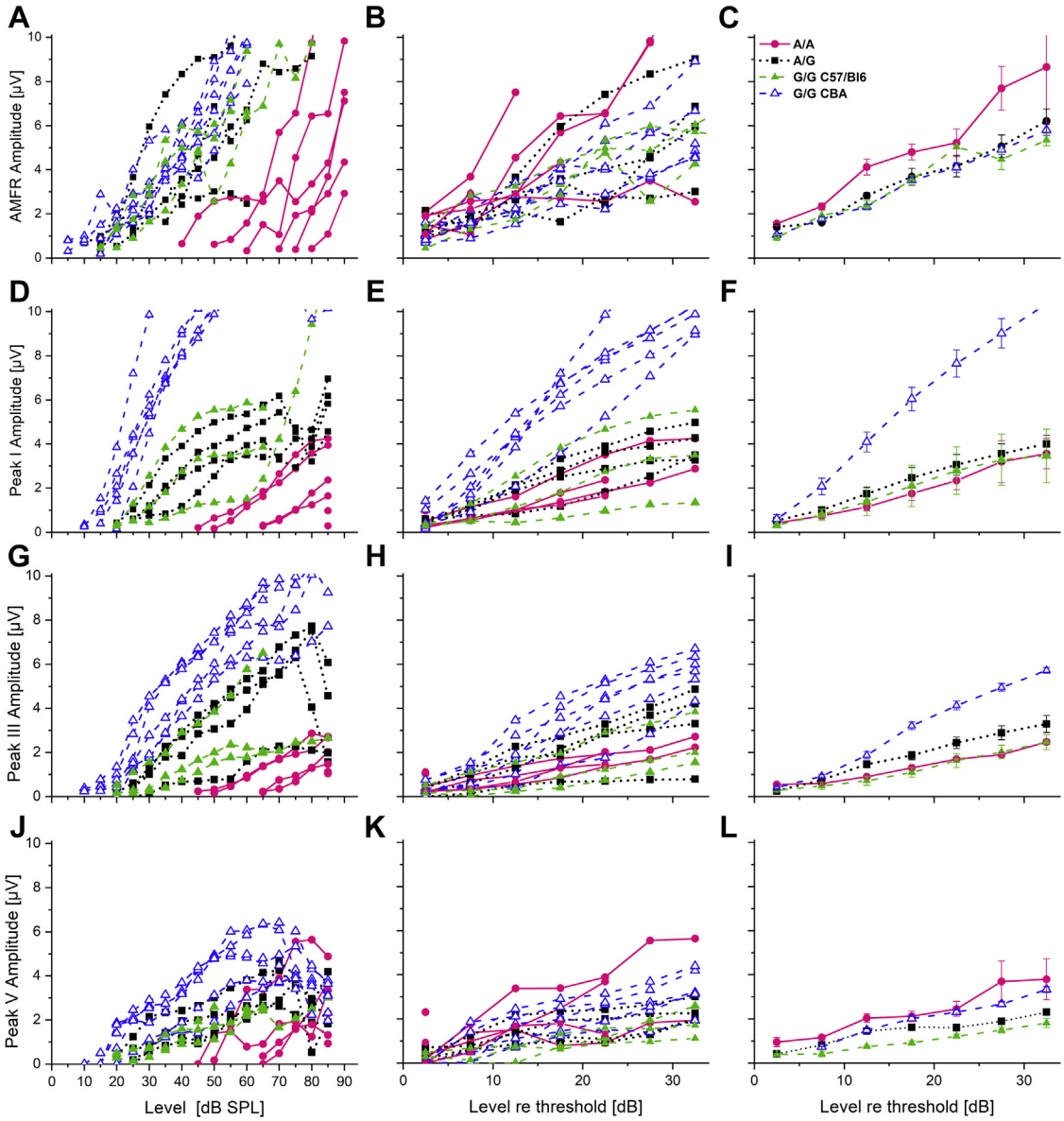

Fig. 6. Amplitude growth functions of different auditory structures show both a genotype and strain-dependent phenotype at one year of age. The left column (A, D, G, J) shows individual amplitude growth functions plotted for stimulus intensity in dB SPL. The middle column (B, E, H, K) shows the growth functions as in the left column plotted for stimulus level respective to threshold (up to 35 dB above threshold). The right column (C, F, I, L) shows the average group data of the corresponding plot in the middle column. (B and C) The amplitude modulation following response (AMFR) growth functions of the one-year-old cohort show a significant influence of genotype with the A/A mice having the highest amplitudes. (E and F) A significant strain-dependent difference can be observed for auditory brainstem response (ABR) wave I, but no difference between the different C57Bl/6 mice. (H and I) For ABR wave III, again the CBA/CaJ mice showed a steeper growth curve than all other mice. (K and L) For peak V, the CBA/J mice show a steeper growth function than both the homozygous G/G C57Bl/6 mice and the heterozygous C57Bl/6 animals, whereas there was no difference to the homozygous A/A mice. Animal numbers, stimulation parameters, color codes, and symbols as in Fig. 5. For the statistical results, see Appendices Table A4-1 (2-way ANOVA), Table A4-2 (Scheffe test for post hoc comparison excluding CBA/J mice), and Table A4-3 (Scheffe test including CBA/J mice).

strain-dependent differences in amplitude growth function are influenced by differences in SGC survival in the 2 strains.

4.3. The heterozygous *Cdh23*$^{735\ A\ >\ G}$ mutation

Mice on a C57BL/6 background, among other strains, are known to have age-related hearing loss beginning at 3 months of age (Bowl and Dawson, 2015), and it is already evident at 5–11 weeks in the present study (Fig. 2). This is unfortunate because the C57BL/6 strain is preferred by the NIH for transgenic experiments (NIH Planning Meeting, 2005) as well as the background strain used by the International Mouse Phenotyping Consortium to create their mutant mouse lines (Simon et al., 2013). The first mutation identified for age-related hearing loss in C57BL/6 mice is *Ahl1*, which is localized at the same position in chromosome 10 as the later identified *Cdh23* gene. *Cdh23* plays a crucial role during the development and maintenance of the hair-bundle and the tip-links. Nonsense mutations in *Cdh23* lead to a disruption in the formation of transient lateral links and kinociliary links during development, resulting in a disarray of the hair bundle and, consequently, to congenital deafness as seen in Usher 1D patients or waltzer mice (Palma et al., 2001). Missense mutations on the other hand are presumed not to interrupt development but to affect the mature tip links (Manji et al., 2011). The point mutation that was the focus of this study leads to an in-frame skipping of exon 7 and is suspected to lead to an increased breakage and reduced repair of the tip links

(Johnson et al., 2017). Presumably, the protein levels of CDH23 missing exon 7 are sufficient even in homozygous animals to allow normal development but are not sufficient to maintain the tip links during aging or noise exposure (Miyasaka et al., 2013). Our findings suggest that the phenotype of heterozygous *Cdh23*$^{735A/G}$ mice also differs from the wild type mice. Our sensitive AMFR testing revealed that by one year of age, the heterozygous *Cdh23*$^{735A/G}$ mice showed a deficit in terms of temporal processing (see Section 4.4), although their hearing thresholds were comparable to wild-type animals.

Our results support the hypothesis that the reduced amount of wild-type Cdh23 protein in the heterozygous animals makes the tip links more vulnerable to breakage or impairs the repair mechanisms. Although the amount of intact tip links is sufficient to retain low hearing thresholds, it is not sufficient to maintain the high level of synchrony needed to faithfully code higher modulations frequencies. Holme and Steel, 2004 also reported a phenotype corresponding to an estimated 50% protein reduction in heterozygous waltzer mice compared with mice homozygous for the wild-type gene. Especially interesting is that this mutation (*Cdh23*^{v}) was also assumed to be recessive, for example, having unaffected carriers (Miyasaka et al., 2013).

4.4. AMFR detected temporal coding deficits in mice heterozygous for Ahl1

The present results show that the heterozygosity of *Cdh23*$^{735A/G}$ did not conserve temporal processing in aged mice. There was a decline in temporal acuity for high modulation frequencies for *Cdh23*$^{735A/G}$ mice at one year in comparison to age-matched *Cdh23*$^{735G/G}$ mice. This deficit in the heterozygous mice has not been reported previously and is in addition to any strain difference between aging C57BL/6 and CBA mice.

If the heterozygous *Cdh23*$^{735A/G}$ mice have more surviving tip links than the homozygous *Cdh23*^{735A} mice, why then do they have worse temporal processing? A study by Indzhykulian et al., 2013 describes the repair mechanism of broken tip links as a two-step process in which only the second step involves CDH23 and restores the adaptation properties of the mechanotransducer channels. It might be that CDH23 missing exon 7 cannot fulfill this task to the same amount as the correctly transcribed protein. As only 50% of the proteins are affected, only some of the tip-links might be affected and this number may increase with age. Slight differences in the structure of some tip links might be just enough to alter the mechanics and timing of tip link movement and introduce internal noise into the system during acoustic stimulation. Internal noise is implicated in the subtle deficits in binaural processing found in human subjects with "normal" hearing (Bernstein and Trahiotis, 2018).

Decreased synchrony or increased internal noise at the level of the hair cells would result in reduced synchrony in the central auditory system (Frisina, 2001). Any change in timing in the brainstem may be more obvious after the convergence of inputs in the IC, the location of our vertex electrode. Studies of temporal processing abilities at the level of single units in the IC also report age-related changes such as higher minimum gap detection thresholds (Walton et al., 1997, 1998). Plasticity in response to the changed input from the cochlea and/or aging per se has been reported at the level of the cochlear nucleus and IC (Chambers et al., 2016; Frisina and Walton, 2006; Walton et al., 2002) and might further contribute to the observed changes in the AMFRs, which include these structures as signal generators. Normally, the IC receives brief, well-timed, transient excitatory synaptic inputs from the auditory brainstem (Kopp-Scheinpflug and Forsythe, 2018; Ono and Oliver, 2014; Rubio, 2018). Such inputs would be necessary to maintain a high level of PS in the midbrain response to modulated stimuli with raised sine envelopes and rapid rise times. Glutamatergic neurons in the IC in particular are well synchronized to the envelope of the raised sine stimulus (Ono et al., 2017). Thus, an increase in internal noise in the timing of the cochlear response to sound may result in a degraded timing signal at the level of the auditory midbrain.

4.5. Functional implications for auditory processing in carriers of mutations

Our findings suggest that although the *Ahl1*/*Cdh23*$^{735\ A>G}$ mutation is reported to only affect homozygous individuals (Noben-Trauth et al., 2003), heterozygous individuals have a less obvious, and therefore, overlooked phenotype. Although all mutations of *Cdh23* in mice have been considered to be recessive (Miyasaka et al., 2013), our findings support the notion that heterozygous "carriers" show a more subtle phenotype than the homozygous animals.

Because mutations of *Cdh23* are involved in human syndromic and nonsyndromic hearing loss, it is likely that the assumingly unaffected carriers might also have auditory deficits. In homozygous individuals, the overall hearing loss may mask additional auditory processing deficits. We postulate that the AMFR method is a powerful tool for the assessment of auditory function in the heterozygous population.

Deficits in temporal processing will cause poor speech recognition (He et al., 2009; Snell et al., 2002; Zeng et al., 1999). Decreased speech intelligibility, especially in noisy environments, is a common phenomenon seen even in older considered "normal hearing" listeners (Füllgrabe et al., 2015; Snell et al., 2002). Although different stations of the auditory system and other factors such as cognitive decline might contribute to this phenomenon (Harris et al., 2010; Kujawa and Liberman, 2009; Xie and Manis, 2017), the very first step in this process is the mechanotransduction in the cochlear hair cells. Studying the subtle changes in heterozygous animal models might shed light on both the physiological and pathophysiological states of this key process in the auditory system.

Acknowledgements

This work was supported by grants HHS | NIH | National Institute on Deafness and Other Communication Disorders (NIDCD) - R21-DC013822 [DLO, ALB] and DOD | United States Army | MEDCOM | Congressionally Directed Medical Research Programs - W81XWH-18-1-0135 [DLO, ALB] and the UConn Health Research Program (NPM).

The authors thank Professor Shigeyuki Kuwada for creating the AMFR method and for his helpful comments and teaching of the AMFR method. The authors also thank Dr. Gongqiang Yu for writing the AMFR program for them.

Appendix A. Supplementary data

Supplementary data to this article can be found online at https://doi.org/10.1016/j.neurobiolaging.2019.02.029.

Disclosure

The authors declare no competing financial interests.

References

Aoyagi, M., Kiren, T., Furuse, H., Fuse, T., Suzuki, Y., Yokota, M., Koike, Y., 1994. Pure-tone threshold prediction by 80-hz amplitude-modulation following response. Acta Otolaryngol. Suppl. 114, 7–14.

Babkoff, H., Fostick, L., 2017. Age-related changes in auditory processing and speech perception: cross-sectional and longitudinal analyses. Eur. J. Ageing 14, 269–281.
Bernstein, L.R., Trahiotis, C., 2018. Effects of interaural delay, center frequency, and no more than "slight" hearing loss on precision of binaural processing: empirical data and quantitative modeling. J. Acoust. Soc. Am. 144, 292.
Bork, J.M., Peters, L.M., Riazuddin, S., Bernstein, S.L., Ahmed, Z.M., Ness, S.L., Polomeno, R., Ramesh, A., Schloss, M., Srisailpathy, C.R., Wayne, S., Bellman, S., Desmukh, D., Ahmed, Z., Khan, S.N., Kaloustian, V.M., Li, X.C., Lalwani, A., Riazuddin, S., Bitner-Glindzicz, M., Nance, W.E., Liu, X.Z., Wistow, G., Smith, R.J., Griffith, A.J., Wilcox, E.R., Friedman, T.B., Morell, R.J., 2001. Usher syndrome 1D and nonsyndromic autosomal recessive deafness DFNB12 are caused by allelic mutations of the novel cadherin-like gene CDH23. Am. J. Hum. Genet. 68, 26–37.
Bowl, M.R., Dawson, S.J., 2015. The mouse as a model for age-related hearing loss - a mini-review. Gerontology 61, 149–157.
Chambers, A.R., Resnik, J., Yuan, Y., Whitton, J.P., Edge, A.S., Liberman, M.C., Polley, D.B., 2016. Central gain restores auditory processing following near-complete cochlear denervation. Neuron 89, 867–879.
Fitzgibbons, P.J., Gordon-Salant, S., 1996. Auditory temporal processing in elderly listeners. J. Am. Acad. Audiol. 7, 183–189.
François, M., Dehan, E., Carlevan, M., Dumont, H., 2016. Use of auditory steady-state responses in children and comparison with other electrophysiological and behavioral tests. Eur. Ann. Otorhinolaryngol. Head Neck Dis. 133, 331–335.
Frisina, R.D., 2001. Subcortical neural coding mechanisms for auditory temporal processing. Hear. Res. 158, 1–27.
Frisina, R.D., Walton, J.P., 2006. Age-related structural and functional changes in the cochlear nucleus. Hearing Res. 216-217, 216–223.
Frisina, R.D., Newman, S.R., Zhu, X., 2007. Auditory efferent activation in CBA mice exceeds that of C57s for varying levels of noise. J. Acoust. Soc. Am. 121, EL29–EL34.
Füllgrabe, C., Moore, B.C.J., Stone, M.A., 2015. Age-group differences in speech identification despite matched audiometrically normal hearing: contributions from auditory temporal processing and cognition. Front. Aging Neurosci. 6, 347.
Gordon-Salant, S., Fitzgibbons, P.J., 1993. Temporal factors and speech recognition performance in young and elderly listeners. J. Speech Hear. Res. 36, 1276–1285.
Griffiths, S.K., Chambers, R.D., 1991. The amplitude modulation-following response as an audiometric tool. Ear Hear. 12, 235–241.
Harris, K.C., Eckert, M.A., Ahlstrom, J.B., Dubno, J.R., 2010. Age-related differences in gap detection: effects of task difficulty and cognitive ability. Hearing Res. 264, 21–29.
He, N.J., Mills, J.H., Ahlstrom, J.B., Dubno, J.R., 2009. Age-related differences in the temporal modulation transfer function with pure-tone carriers. J. Acoust. Soc. Am. 124, 3841–3849.
Hequembourg, S., Liberman, M.C., 2001. Spiral ligament pathology: a major aspect of age-related cochlear degeneration in C57BL/6 mice. J. Assoc. Res. Otolaryngol. 2, 118–129.
Hickox, A.E., Liberman, M.C., 2014. Is noise-induced cochlear neuropathy key to the generation of hyperacusis or tinnitus? J. Neurophysiol. 111, 552–564.
Holme, R.H., Steel, K.P., 2004. Progressive hearing loss and increased susceptibility to noise-induced hearing loss in mice carrying a Cdh23 but not a Myo7a mutation. J. Assoc. Res. Otolaryngol. 5, 66–79.
Indzhykulian, A.A., Stepanyan, R., Nelina, A., Spinelli, K.J., Ahmed, Z.M., Belyantseva, I.A., Friedman, T.B., Barr-Gillespie, P.G., Frolenkov, G.I., 2013. Molecular remodeling of tip links underlies mechanosensory regeneration in auditory hair cells. PLoS Biol. 11, e1001583.
Johnson, K.R., Erway, L.C., Cook, S.A., Willott, J.F., Zheng, Q.Y., 1997. A major gene affecting age-related hearing loss in C57BL/6J mice. Hearing Res. 114, 83–92.
Johnson, K.R., Tian, C., Gagnon, L.H., Jiang, H., Ding, D., Salvi, R., 2017. Effects of Cdh23 single nucleotide substitutions on age-related hearing loss in C57BL/6 and 129S1/Sv mice and comparisons with congenic strains. Sci. Rep. 7, 44450.
Kim, B.J., Kim, A.R., Lee, C., Kim, S.Y., Kim, N.K.D., Chang, M.Y., Rhee, J., Park, M.H., Koo, S.K., Kim, M.Y., Han, J.H., Oh, S.H., Park, W.Y., Choi, B.Y., 2016. Discovery of CDH23 as a significant contributor to progressive postlingual sensorineural hearing loss in Koreans. PLoS One 11, e0165680.
Kopp-Scheinpflug, C., Forsythe, I.D., 2018. Integration of synaptic and intrinsic conductances shapes microcircuits in the superior olivary complex. In: Oliver, D.L., Cant, N.B., Fay, R.R., Popper, A.N. (Eds.), The Mammalian Auditory Pathways: Synaptic Organization and Microcircuits. Springer International Publishing, Cham, pp. 101–126.
Kujawa, S.G., Liberman, M.C., 2009. Adding insult to injury: cochlear nerve degeneration after "temporary" noise-induced hearing loss. J. Neurosci. 29, 14077–14085.
Kuwada, S., Batra, R., Maher, V.L., 1986. Scalp potentials of normal and hearing-impaired subjects in response to sinusoidally amplitude-modulated tones. Hear. Res. 21, 179–192.
Kuwada, S., Anderson, J.S., Batra, R., Fitzpatrick, D.C., Teissier, N., D'Angelo, W.R., 2002. Sources of the scalp-recorded amplitude-modulation following response. J. Am. Acad. Audiol. 13, 188–204.
Manji, S.S., Miller, K.A., Williams, L.H., Andreasen, L., Siboe, M., Rose, E., Bahlo, M., Kuiper, M., Dahl, H.H., 2011. An ENU-induced mutation of Cdh23 causes congenital hearing loss, but no vestibular dysfunction, in mice. Am. J. Pathol. 179, 903–914.
Miyasaka, Y., Suzuki, S., Ohshiba, Y., Watanabe, K., Sagara, Y., Yasuda, S.P., Matsuoka, K., Shitara, H., Yonekawa, H., Kominami, R., Kikkawa, Y., 2013. Compound heterozygosity of the functionally null cdh23(v-ngt) and hypomorphic cdh23(ahl) alleles leads to early-onset progressive hearing loss in mice. Exp. Anim. 62, 333–346.
Müller, U., 2008. Cadherins and mechanotransduction by hair cells. Curr. Opin. Cell Biol. 20, 557–566.
NIH Planning Meeting for a Knockout Mouse Project, 2005. https://www.genome.gov/15014549/nih-planning-meeting-for-knockout-mouse-project. (Accessed 9 July 2018).
Noben-Trauth, K., Zheng, Q.Y., Johnson, K.R., 2003. Association of cadherin 23 with polygenic inheritance and genetic modification of sensorineural hearing loss. Nat. Genet. 35, 21–23.
Ono, M., Oliver, D.L., 2014. Asymmetric temporal interactions of sound-evoked excitatory and inhibitory inputs in the mouse auditory midbrain. J. Physiol. 592, 3647–3669.
Ono, M., Bishop, D.C., Oliver, D.L., 2017. Identified GABAergic and glutamatergic neurons in the mouse inferior colliculus share similar response properties. J. Neurosci. 37, 8952–8964.
Palma, F.D., Holme, R.H., Bryda, E.C., Belyantseva, I.A., Pellegrino, R., Kachar, B., Steel, K.P., Noben-Trauth, K., 2001. Mutations in Cdh23, encoding a new type of cadherin, cause stereocilia disorganization in waltzer, the mouse model for Usher syndrome type 1D. Nat. Genet. 27, 103–107.
Parthasarathy, A., Herrmann, B., Bartlett, E.L., 2019. Aging alters envelope representations of speech-like sounds in the inferior colliculus. Neurobiol. Aging 73, 30–40.
Purcell, D.W., John, S.M., Schneider, B.A., Picton, T.W., 2004. Human temporal auditory acuity as assessed by envelope following responses. J. Acoust. Soc. Am. 116, 3581–3593.
Radziwon, K.E., June, K.M., Stolzberg, D.J., Xu-Friedman, M.A., Salvi, R.J., Dent, M.L., 2009. Behaviorally measured audiograms and gap detection thresholds in CBA/CaJ mice. J. Comp. Physiol. A. Neuroethol. Sens. Neural Behav. Physiol. 195, 961–969.
Robert Frisina, D., Frisina, R.D., 1997. Speech recognition in noise and presbycusis: relations to possible neural mechanisms. Hearing Res. 106, 95–104.
Rubio, M.E., 2018. Microcircuits of the ventral cochlear nucleus. In: Oliver, D.L., Cant, N.B., Fay, R.R., Popper, A.N. (Eds.), The Mammalian Auditory Pathways: Synaptic Organization and Microcircuits. Springer International Publishing, Cham, pp. 41–71.
Rutherford, B.R., Brewster, K., Golub, J.S., Kim, A.H., Roose, S.P., 2018. Sensation and psychiatry: linking age-related hearing loss to late-life depression and cognitive decline. Am. J. Psychiatry 175, 215–224.
Sergeyenko, Y., Lall, K., Charles Liberman, M., Kujawa, S.G., 2013. Age-related cochlear synaptopathy: an early-onset contributor to auditory functional decline. J. Neurosci. 33, 13686–13694.
Simon, M.M., Greenaway, S., White, J.K., Fuchs, H., Gailus-Durner, V., Wells, S., Sorg, T., Wong, K., Bedu, E., Cartwright, E.J., Dacquin, R., Djebali, S., Estabel, J., Graw, J., Ingham, N.J., Jackson, I.J., Lengeling, A., Mandillo, S., Marve, J., Meziane, H., Preitner, F., Puk, O., Roux, M., Adams, D.J., Atkins, S., Ayadi, A., Becker, L., Blake, A., Brooker, D., Cater, H., Champy, M.F., Combe, R., Danecek, P., Di Fenza, A., Gates, H., Gerdin, A.K., Golini, E., Hancock, J.M., Hans, W., Hölter, S.M., Hough, T., Jurdic, P., Keane, T.M., Morgan, H., Müller, W., Neff, F., Nicholson, G., Pasche, B., Roberson, L.A., Rozman, J., Sanderson, M., Santos, L., Selloum, M., Shannon, C., Southwel, A., Tocchini-Valentini, G.P., Vancollie, V.E., Westerberg, H., Wurst, W., Zi, M., Yalcin, B., Ramirez-Solis, R., Steel, K.P., Mallon, A.M., De Angelis, M.H., Herault, Y., Brown, S.D.M., 2013. A comparative phenotypic and genomic analysis of C57BL/6J and C57BL/6N mouse strains. Genome Biol. 14, R82.
Snell, K.B., Mapes, F.M., Hickman, E.D., Frisina, D.R., 2002. Word recognition in competing babble and the effects of age, temporal processing, and absolute sensitivity. J. Acoust. Soc. Am. 112, 720–727.
Walton, J.P., Frisina, R.D., Ison, J.R., O'Neill, W.E., 1997. Neural correlates of behavioral gap detection in the inferior colliculus of the young CBA mouse. J. Comp. Physiol. A. 181, 161–176.
Walton, J.P., Frisina, R.D., O'Neill, W.E., 1998. Age-related alteration in processing of temporal sound features in the auditory midbrain of the CBA mouse. J. Neurosci. 18, 2764.
Walton, J.P., Simon, H., Frisina, R.D., Giraudet, P., 2002. Age-related alterations in the neural coding of envelope periodicities. J. Neurophysiol. 88, 565–578.
Williamson, T.T., Zhu, X., Walton, J.P., Frisina, R.D., 2015. Auditory brainstem gap responses start to decline in mice in middle age: a novel physiological biomarker for age-related hearing loss. Cell Tissue Res. 361, 359–369.
Xie, R., Manis, P.B., 2017. Synaptic transmission at the endbulb of Held deteriorates during age-related hearing loss. J. Physiol. 595, 919–934.
Zeng, F.-G., Oba, S., Garde, S., Sininger, Y., Starr, A., 1999. Temporal and speech processing deficits in auditory neuropathy. Neuroreport 10, 3429–3435.